UNCERTAINTY PRINCIPLES FOR SIGNALS DEFINED ON GRAPHS: BOUNDS AND CHARACTERIZATIONS

Ameya Agaskar and Yue M. Lu

Harvard School of Engineering and Applied Sciences
Cambridge, MA 02138, USA
Email: {aagaskar, yuelu}@seas.harvard.edu

ABSTRACT

The classical uncertainty principle provides a fundamental tradeoff in the localization of a signal in the time and frequency domains. In this paper we describe a similar tradeoff for signals defined on graphs. We describe the notions of "spread" in the graph and spectral domains, using the eigenvectors of the graph Laplacian as a surrogate Fourier basis. We then describe how to find signals that, among all signals with the same spectral spread, have the smallest graph spread about a given vertex. For every possible spectral spread, the desired signal is the solution to an eigenvalue problem. Since localization in graph and spectral domains is a desirable property of the elements of wavelet frames on graphs, we compare the performance of some existing wavelet transforms to the obtained bound.

***Index Terms*—** Signal processing on graphs, uncertainty principles, wavelets, graph Laplacians, spectral graph theory

1. INTRODUCTION

The *uncertainty principle* is a cornerstone result in time-frequency signal processing and harmonic analysis. It limits the degree to which a signal can be simultaneously localized in time and frequency. More precisely, let $x(t) \in \mathcal{L}^2(\mathbb{R})$ be a real-valued signal with norm $||x||$ (in this work we will only refer to the $\mathcal{L}^2$ norm) and Fourier transform $\widehat{x}(\omega)$. We use [1]

$$\Delta_t^2 \stackrel{\text{def}}{=} \frac{1}{||x||^2}\int_{-\infty}^{\infty}(t-t_0)^2|x(t)|^2dt,$$
$$\Delta_\omega^2 \stackrel{\text{def}}{=} \frac{1}{||x||^2}\int_{-\infty}^{\infty}\omega^2|\widehat{x}(\omega)|^2\frac{d\omega}{2\pi}$$

to measure the "spreads" of $x(t)$ in time and frequency, respectively, with $t_0 \stackrel{\text{def}}{=} \frac{1}{||x||^2}\int_{-\infty}^{\infty} t|x(t)|^2dt$. The uncertainty principle states that

$$\Delta_t^2\,\Delta_\omega^2 \geq \frac{1}{4}, \tag{1}$$

which implies that localizing a signal in one domain must be done at the cost of increased spread in the other domain.

In this paper, we establish analogous uncertainty principles for signals defined on graphs. In recent years, there has been rapidly growing interest in extending traditional signal processing theory from standard domains [*e.g.*, $\ell^2(\mathbb{Z}^d)$] to non-standard domains such as graphs, which can be used to model communication networks, to approximate manifolds [2, 3], or even to capture nonlocal self-similarity structures in images [4].

A. Agaskar is also with MIT Lincoln Laboratory. This work was sponsored by the Department of the Air Force under Contract FA8721-05-C-0002. Opinions, interpretations, conclusions and recommendations are those of the authors and are not necessarily endorsed by the United States Government.

Early work in this direction focused on multiscale representations of meshes for computer graphics applications [5]. Another line of work examined the use of graph approximations to manifolds, with Belkin and later Giné and Koltchinskii examining the role of the graph Laplacians [2, 3]. More recently, several authors began considering multiscale wavelet-like transforms on graphs [6]–[9]. When designing wavelet frames and bases on graphs, it is desirable that the basis functions be well-localized on the graph, and well-localized in the "frequency" domain (where frequency is defined in terms of the eigenvalues of the Laplacian matrix, which is defined in Section 2.2).

In a recent work [10] we introduced the notions of graph and spectral spreads $\Delta_g^2(\boldsymbol{x})$ and $\Delta_s^2(\boldsymbol{x})$ that allow us to quantify exactly how well-localized a signal $\boldsymbol{x}$ is in both graph and spectral domains. In that work, we also bounded the product $\Delta_g^2\Delta_s^2$ from below, in analogy to the classical time-frequency uncertainty principle in (1). However, the bound was not tight, and required constraints on the graph and the signal under consideration.

The are two main contributions of this work: First, we provide a complete characterization of the feasibility region in the space of possible pairs $(\Delta_s^2(\boldsymbol{x}), \Delta_{g,u_0}^2(\boldsymbol{x})^2)$ achievable by some signal $\boldsymbol{x}$, where Δ_{g,u_0}^2 is the graph spread centered at some nominal center vertex u_0. Second, we describe how to implicitly compute a function of the form

$$\gamma(s) = \min_{\boldsymbol{x}}\ \Delta_{g,u_0}^2(\boldsymbol{x})\ \text{ subject to } \Delta_s^2(\boldsymbol{x}) = s.$$

This function is important because it forms the lower boundary of the feasibility region. A main result in this paper is to show that each point on the curve $\gamma(s)$ is achievable by an eigenvector of a particular Hermitian matrix pencil, and vice versa. The computational procedure for finding the curve $\gamma(s)$ then boils down to a sequence of eigenvalue problems.

The rest of the paper is organized as follows. In Section 2 we provide the mathematical background for spectral analysis on graphs. In Section 3 we describe the feasibility region of the space of possible pairs of spreads, and describe a computational procedure for finding the lower boundary of the region. To verify the theoretical results developed in this work, we show in Section 4 the resulting curve for a graph constructed from a smooth manifold and compare the performance of existing wavelet constructions in the literature to the computed bound. We conclude the paper in Section 5. Due to space limitations, we only present the proofs for the most important results in this paper, and leave the proofs for all other results to [11].

2. MATHEMATICAL FORMULATION

2.1. Graphs, Signals, and Notation

We begin with a simple, undirected graph $G = (V(G), E(G))$, where $V(G) = \{v_1, v_2, \ldots, v_N\}$ is the set of N vertices and $E(G) = \{e_1, e_2, \ldots, e_M\}$ is the set of M edges. Each edge is of the form

$e = \{u, v\}$, with $u, v \in V$; an edge is an unordered pair of vertices. The graph is *simple* in that is has no loops, or edges connecting a vertex to itself; the graph is undirected because the edges have no orientation. We will use the notation $u \sim v$ to indicate that u and v are connected by an edge. The graph is uniquely determined by its adjacency matrix $\boldsymbol{A} = [a_{ij}]_{ij}$, where $a_{ij} = 1$ if there is a link between v_i and v_j, and $a_{ij} = 0$ otherwise. The diagonal of $\boldsymbol{A}$ is zero because no loops are allowed, and $\boldsymbol{A}$ is symmetric because the graph is undirected. A simple generalization is a weighted graph, where each edge has a "weight," and the entries of the adjacency matrix are replaced by the weights of the corresponding edges.

The degree of a vertex $\delta(v), v \in V$ is the number of edges incident upon that vertex. It is equal to the sum of the entries of $\boldsymbol{A}$ in the row or column corresponding to that vertex. We define $\boldsymbol{D}$ as the diagonal matrix that has the vertex degrees on the diagonal. We can also define a distance function on the graph: $d(u, v)$ is the smallest number of edges in a path connecting vertex u to vertex v. It satisfies all the properties of a metric. We will define $\delta_k(v)$ as the number of vertices on the graph a distance k from the v, with $\delta_1(v) = \delta(v)$. The eccentricity of a vertex $\epsilon(v)$ is the distance to the vertex on the graph furthest from v.

For every vertex u on the graph, we define

$$\boldsymbol{P}_u \stackrel{\text{def}}{=} \text{diag}\left\{d(u, v_1), d(u, v_2), \ldots, d(u, v_N)\right\} \tag{2}$$

as the diagonal matrix of distances to u. This matrix will become important when we define the spread of a signal on a graph.

A signal on the graph $\boldsymbol{x} \in \ell^2(G)$ is a mapping from the set of vertices to $\mathbb{R}$. It can be treated as a vector in $\mathbb{R}^N$, and so any such signal will be denoted by a boldface variable. There is a natural inner product on $\ell^2(G)$ defined by $\langle \boldsymbol{x}, \boldsymbol{y} \rangle = \boldsymbol{y}^T \boldsymbol{x}$, which induces a norm $||\boldsymbol{x}|| = \sqrt{\boldsymbol{x}^T \boldsymbol{x}}$. We will denote the value of $\boldsymbol{x}$ at vertex v by $x(v)$.

2.2. Spectral Graph Theory and Fourier Transforms on Graphs

Spectral graph theory relates the properties of graphs to the eigenvalues of certain linear operators related to the graph [12]. These operators transform a signal on the graph to a different signal on the graph. Any linear operator on $\ell^2(G)$ can be represented by an $N \times N$ matrix. The operator most commonly considered in spectral graph theory is the Laplacian matrix, given by

$$\boldsymbol{L} \stackrel{\text{def}}{=} \boldsymbol{I} - \boldsymbol{D}^{-1/2} \boldsymbol{A} \boldsymbol{D}^{-1/2}.$$

This is the so-called "normalized" Laplacian. There is also an unnormalized version of the Laplacian, but we consider only the normalized version here for simplicity. The Laplacian is a symmetric, positive semidefinite matrix. A connected graph has the eigenvalue 0 with multiplicity 1, corresponding to a unit-norm eigenvector $\boldsymbol{x}_0$ defined by $x_0(v) = \sqrt{\frac{\delta(v)}{2M}}$. The maximum possible eigenvalue is 2, attained only by bipartite graphs. The Laplacian matrix is analogous to the Laplacian operator $-\nabla^2$ or $-\frac{d^2}{dx^2}$ on the real line. In fact, it provides the standard stencil approximation for the operator on a lattice discretization.

Since the Laplacian matrix is symmetric, we can diagonalize it as

$$\boldsymbol{L} = \boldsymbol{F} \boldsymbol{\Lambda} \boldsymbol{F}^T,$$

where $\boldsymbol{F}$ is the matrix whose columns are the eigenvectors of $\boldsymbol{L}$, and $\boldsymbol{\Lambda}$ is the diagonal matrix of $\boldsymbol{L}$'s eigenvalues. Given a vector $\boldsymbol{x}$, we might like to find its representation in terms of the eigenvectors of $\boldsymbol{L}$. This can be computed by taking

$$\widehat{\boldsymbol{x}} = \boldsymbol{F}^T \boldsymbol{x},$$

where we call $\widehat{\boldsymbol{x}}$ the *graph Fourier transform* of $\boldsymbol{x}$. The matrix $\boldsymbol{F}^T$ is the Fourier transform operator. Since the Laplacian is symmetric, $\boldsymbol{F}$ is orthogonal, so $\boldsymbol{F}\boldsymbol{F}^T = \boldsymbol{F}^T\boldsymbol{F} = \boldsymbol{I}$. (Of course, if there are repeated eigenvalues, then the columns spanning the eigenspace of a repeated eigenvalue need not be orthogonal, but $\boldsymbol{F}$ can always be chosen to be orthogonal.) It follows that we can invert the Fourier transform:

$$\boldsymbol{x} = \boldsymbol{F} \widehat{\boldsymbol{x}}.$$

2.3. Graph and Spectral Spreads

In the classical uncertainty principle for signals defined on the real line, the time spread for a signal $x(t)$ is defined by

$$\Delta_t^2 = \min_{t_0} \frac{1}{||x||^2} \int (t - t_0)^2 |x(t)|^2 dt.$$

By analogy, we can define the graph spread of a signal $\boldsymbol{x} \in \ell^2(G)$ as

$$\begin{aligned} \Delta_g^2(\boldsymbol{x}) &\stackrel{\text{def}}{=} \min_{u_0} \frac{1}{||\boldsymbol{x}||^2} \sum_{v \in V} d(v, u_0)^2 x(v)^2 \\ &= \min_{u_0} \frac{1}{||\boldsymbol{x}||^2} \boldsymbol{x}^T \boldsymbol{P}_{u_0}^2 \boldsymbol{x}, \end{aligned} \tag{3}$$

where the distance metric $d(\cdot, \cdot)$ is described in Section 2.1, and the matrix $\boldsymbol{P}_{u_0}$ is defined in (2). In the design of wavelet-like transforms on graphs, it is desirable for each basis or frame element to be centered at a *given* vertex, and well-localized on the graph and in the spectral domain. To measure how well a signal is localized about a particular vertex u_0, we define the *localized graph spread* as

$$\begin{aligned} \Delta_{g,u_0}^2(\boldsymbol{x}) &\stackrel{\text{def}}{=} \sum_{v \in V} d(v, u_0)^2 x(v)^2 \\ &= \boldsymbol{x}^T \boldsymbol{P}_{u_0}^2 \boldsymbol{x}. \end{aligned} \tag{4}$$

Meanwhile, the frequency spread of a signal $x(t)$ is defined by

$$\begin{aligned} \Delta_\omega^2 &= \frac{1}{||x||^2} \int \omega^2 |\widehat{x}(\omega)|^2 \frac{d\omega}{2\pi} \\ &= \frac{1}{||x||^2} \int x(t) \frac{-d^2}{dt^2} x(t) dt \end{aligned}$$

Since the graph Laplacian is analogous to the Laplacian operator $\frac{-d^2}{dt^2}$, we can define the spectral spread of $\boldsymbol{x}$ as

$$\Delta_s^2(x) = \frac{1}{||\boldsymbol{x}||^2} \boldsymbol{x}^T \boldsymbol{L} \boldsymbol{x}. \tag{5}$$

We refer the readers to [10] for more justifications for using (5) as the graph spectral spread. Finally, we note that all the spreads defined in (3), (4), and (5) are invariant to scaling transforms.

3. UNCERTAINTY PRINCIPLES: BOUNDS AND CHARACTERIZATIONS

3.1. Feasible Regions

In general, we are interested in the feasible region

$$\mathcal{D} \stackrel{\text{def}}{=} \left\{(s, g) : \Delta_s^2(\boldsymbol{x}) = s, \Delta_{g,u_0}(\boldsymbol{x}) = g \text{ for some } \boldsymbol{x} \in \ell^2(G)\right\}. \tag{6}$$

We can easily verify the following properties:

1. The set $\mathcal{D}$ is a closed subset of $[0, \lambda_{\max}(\boldsymbol{L})] \times [0, \epsilon(u_0)^2]$, where $\lambda_{\max}$ is the largest eigenvalue, and $\epsilon(u_0)$ is the eccentricity of the vertex u_0.

2. The points $(1, 0)$, corresponding to an impulse at u_0, and $(0, \boldsymbol{x}_0^T P_{u_0}^2 \boldsymbol{x}_0)$, where $\boldsymbol{x}_0$ is the vector defined in Section 2.2 belong to $\mathcal{D}$. In fact, they are exactly the points where $\mathcal{D}$ intersects with the horizontal and vertical axes, respectively.

The following proposition points to a more fundamental property:

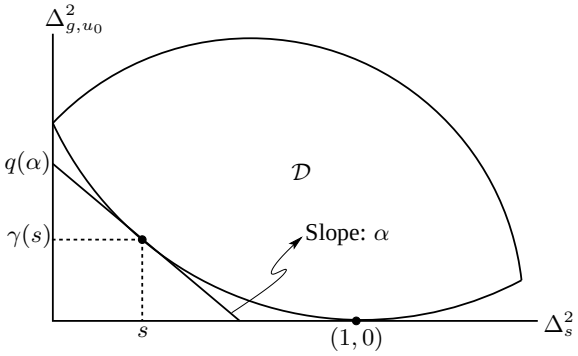

Fig. 1. A characterization of the feasible region $\mathcal{D}$ for the spectral and graph spreads. $\mathcal{D}$ is a bounded and convex set, and it intersects the horizontal (and vertical) axis at exactly one point. The lower boundary of $\mathcal{D}$ can be implicitly computed by considering tangent lines of varying slopes.

Proposition 1. *The set $\mathcal{D}$ is convex.*

We leave the proof to [11]. Proposition 1 tells us that $\mathcal{D}$ can be completely characterized by its upper and lower boundaries: any pair between the two boundaries must also be achievable. In this paper, we will describe a technique for finding the lower boundary. A similar technique can be used to find the upper boundary. However, the lower boundary is more interesting because it provides a kind of uncertainty bound for signals on the graph.

3.2. The Lower Boundary of the Feasible Region

In what follows, we describe a parameterization and computational procedure for finding the lower boundary of $\mathcal{D}$.

Definition 1. *The lower boundary curve of $\mathcal{D}$ is*

$$\begin{aligned}\gamma(s) &\stackrel{def}{=} \min_{\boldsymbol{x}} \Delta^2_{g,u_0}(\boldsymbol{x}) \text{ subject to } \Delta^2_s(\boldsymbol{x}) = s \\ &= \min \boldsymbol{x}^T \boldsymbol{P}^2_{u_0} \boldsymbol{x} \text{ subject to } \boldsymbol{x}^T\boldsymbol{x} = 1 \text{ and } \boldsymbol{x}^T L \boldsymbol{x} = s\end{aligned}$$

for all $s \in [0, \lambda_{\max}(\boldsymbol{L})]$.

Using Lagrange multipliers, we can see that if a signal $\boldsymbol{x}$ achieves the minimum for this problem, it must satisfy the equation

$$(\boldsymbol{P}^2_{u_0} + \alpha \boldsymbol{L})\boldsymbol{x} = \lambda \boldsymbol{x}$$

for some real Lagrange multipliers α and λ. If we treat α as being fixed, then this is an eigenvector problem. To study the curve, we define the matrix pencil

$$\boldsymbol{M}(\alpha) \stackrel{\text{def}}{=} \boldsymbol{P}^2_{u_0} + \alpha \boldsymbol{L}$$

and the function

$$q(\alpha) \stackrel{\text{def}}{=} \lambda_{\min}(\boldsymbol{M}(\alpha)).$$

It is easy to see that for any unit norm vector $\boldsymbol{w}$,

$$\Delta^2_{g,u_0} + \alpha \Delta^2_s = \boldsymbol{w}^T (P^2_{u_0} + \alpha L)\boldsymbol{w} \geq q(\alpha). \tag{7}$$

The equation $\Delta^2_{g,u_0} + \alpha\Delta^2_s \geq q(\alpha)$, for any α, defines a half-plane in which $\mathcal{D}$ must lie. This geometric interpretation is illustrated in Figure 1, where a line of slope α provides a lower bound to $\mathcal{D}$. In fact, $\mathcal{D}$ must be contained within the intersection of the half-planes defined by every $\alpha \in (-\infty, \infty)$.

If $\boldsymbol{x}$ is a unit norm eigenvector associated with the smallest eigenvalue, so that

$$(\boldsymbol{P}^2_{u_0} + \alpha \boldsymbol{L})\boldsymbol{x} = q(\alpha)\boldsymbol{x},$$

then $\gamma(\boldsymbol{x}^T \boldsymbol{L} \boldsymbol{x}) = \boldsymbol{x}^T \boldsymbol{P}^2_{u_0} \boldsymbol{x}$. If this were not the case, and thus there were some unit norm $\boldsymbol{w}$ with $\Delta^2_s(\boldsymbol{w}) = \Delta^2_s(\boldsymbol{x})$ and $\Delta^2_{g,u_0}(\boldsymbol{w}) < \Delta^2_{g,u_0}(\boldsymbol{x})$, then we would have

$$\boldsymbol{w}^T(\boldsymbol{P}^2_{u_0} + \alpha \boldsymbol{L})\boldsymbol{w} < \boldsymbol{x}^T(\boldsymbol{P}^2_{u_0} + \alpha \boldsymbol{L})\boldsymbol{x} = q(\alpha), \tag{8}$$

and $\boldsymbol{w}$ would be violating (7).

Following the above argument, any eigenvector of $\boldsymbol{M}(\alpha)$ associated with the eigenvalue $q(\alpha)$ generates a point on the curve $\gamma(\cdot)$. If for some α_0 the multiplicity of the smallest eigenvalue of $\boldsymbol{M}(\alpha)$ is one, then there is exactly one point on the line

$$\Delta^2_{g,u_0} + \alpha_0 \Delta^2_s = q(\alpha_0)$$

that is in $\mathcal{D}$; in this case, the line is tangent to the $\gamma(\cdot)$ curve, as illustrated in Figure 1.

Furthermore, by the Gershgorin disc theorem, there is a neighborhood $\mathcal{N}$ around α_0 on which $\boldsymbol{M}(\alpha)$ has is an eigenvalue near $q(\alpha_0)$ for $\alpha \in \mathcal{N}$, and all other eigenvalues are bounded away from $q(\alpha)$. This combined with standard perturbation results tells us that $q(\alpha)$ is smooth at α_0 [13]. Furthermore, there is a smooth function $\boldsymbol{x}(\alpha)$ defined on $\mathcal{N}$ such that $\boldsymbol{M}(\alpha)\boldsymbol{x}(\alpha) = q(\alpha)\boldsymbol{x}(\alpha)$. Since $\boldsymbol{x}(\alpha)^T\boldsymbol{x}(\alpha) = 1$, we have that $\boldsymbol{x}(\alpha)^T \frac{dv}{d\alpha} = 0$. This allows us to compute an expression for the derivative

$$\left.\frac{dq}{d\alpha}\right|_{\alpha_0} = \boldsymbol{x}(\alpha_0)^T \boldsymbol{L} \boldsymbol{x}(\alpha_0).$$

If the multiplicity is greater than one at α_0, then any vector in the eigenspace is on the curve. Using more complicated Gershgorin/perturbation arguments, we can see that though $q(\alpha)$ is not differentiable at α_0, it has distinct left and right-hand derivatives

$$\left.\frac{dq}{d\alpha}\right|_{\alpha_0^-} = \boldsymbol{x}(\alpha_0^-)^T \boldsymbol{L} \boldsymbol{x}(\alpha_0^-) \text{ and } \left.\frac{dq}{d\alpha}\right|_{\alpha_0^+} = \boldsymbol{x}(\alpha_0^+)^T \boldsymbol{L} \boldsymbol{x}(\alpha_0^+).$$

where

$$\begin{aligned}\boldsymbol{x}(\alpha_0^-) = \max_{\boldsymbol{x}} \boldsymbol{x}^T L \boldsymbol{x} \\ \text{subject to } ||\boldsymbol{x}|| = 1 \text{ and } \boldsymbol{M}(\alpha_0)\boldsymbol{x} = q(\alpha_0)\boldsymbol{x}\end{aligned}$$

and

$$\begin{aligned}\boldsymbol{x}(\alpha_0^+) = \min_{\boldsymbol{x}} \boldsymbol{x}^T L \boldsymbol{x} \\ \text{subject to } ||\boldsymbol{x}|| = 1 \text{ and } \boldsymbol{M}(\alpha_0)\boldsymbol{x} = q(\alpha_0)\boldsymbol{x}.\end{aligned}$$

The eigenvectors $\boldsymbol{x}(\alpha_0^+)$ and $\boldsymbol{x}(\alpha_0^-)$ each generate points on the curve, and it can be shown that every pair on the line segment joining them is achievable as well. Returning to the case of multiplicity one, we will define $\boldsymbol{x}(\alpha_0^+) = \boldsymbol{x}(\alpha^-) = \left.\frac{dq}{d\alpha}\right|_{\alpha_0}$.

Combining these results, we can prove the following theorem.

Theorem 1. *For any $s \in [0, \lambda_{\max}(\boldsymbol{L})]$, the function $\gamma(s) = r$ if any only if there is some $\alpha \in \mathbb{R}$ and $\theta \in [0, 1]$ for which*

$$s = \theta \left.\frac{dq}{d\alpha}\right|_{\alpha^-} + (1-\theta) \left.\frac{dq}{d\alpha}\right|_{\alpha^+}$$

and

$$r = q(\alpha) - \alpha \left(\theta \left.\frac{dq}{d\alpha}\right|_{\alpha^-} + (1-\theta) \left.\frac{dq}{d\alpha}\right|_{\alpha^+} \right).$$

Remark 1. *The result of this theorem implies that we can generate the entire curve $\gamma(\cdot)$ by simply sweeping over $\alpha \in (-\infty, \infty)$; every point on the curve is achievable by an eigenvector, and so the bound is tight. Furthermore, since the set of αs for which the multiplicity of $q(\alpha)$ is greater than one has measure zero, when we do our sweep it is most likely that every iteration will give us a single point on the curve.*

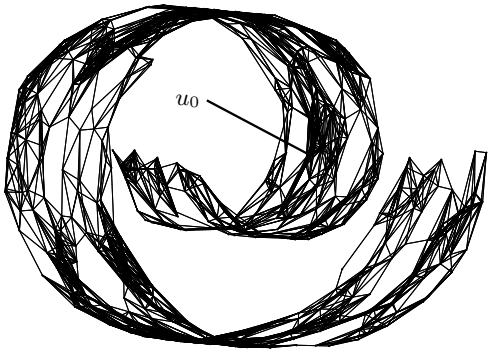

Fig. 2. Swiss roll graph from SGWT toolbox [8]. Samples are chosen uniformly from the swiss roll manifold, and edges are drawn between any vertices within some radius r in $\mathbb{R}^3$ of each other. The vertex u_0 is indicated.

Proof. The "if" direction follows from the geometric arguments above. The "only if" statement is more complicated. From the previous arguments, we can see that on any segment of α-parameters over which the multiplicity of $q(\alpha)$ is one, the x-coordinate of the point generated by the associated eigenvector is continuous. Meanwhile, at the discontinuities (which correspond to those α-parameters with higher multiplicity, we can bridge the gap by taking a convex combination of the multiple eigenvectors. Since $\alpha = \infty$ generates the point with x-coordinate 0, and $\alpha = -\infty$ generates the point with x-coordinate $\lambda_{\max}$, we can find the point $(s, \gamma(s))$ for any $s \in [0, \lambda_{\max}]$. □

4. NUMERICAL RESULTS

To obtain numerical results, we used a graph based on the "Swiss roll" manifold defined in the SGWT toolbox [8]. The graph was generated by picking 500 points uniformly at random from the manifold as vertices. Edges were formed between vertices within a small radius $r = 0.30$ of each other in the manifold's embedding in $\mathbb{R}^3$. The graph and its manifold structure are illustrated in Figure 2.

Based on this graph, spectral graph analysis wavelets [8] and diffusion analysis wavelets [6] were generated. While the spectral graph wavelet transform does not involve downsampling the graph, the diffusion wavelet transform does. The center vertex u_0 was chosen to be one of the vertices that remained in the downsampled graph of the highest level of the diffusion wavelet transform.

To form the lower bound curve, the eigenvector v corresponding to the smallest eigenvalue of $(1-\beta)P_{u_0}^2 + \beta L$ was found for $\beta \in [0, 1]$. This is the same as the eigenvector corresponding to the smallest eigenvalue of $P_{u_0}^2 + \alpha L$, where $\alpha = \frac{\beta}{1-\beta}$; this alternate formulation was used to avoid numerical difficulties at high values of α and was used to trace the curve for all positive values of α. The eigenvector v was used to directly compute a point on the curve: $(\Delta_s^2(v), \Delta_{g,u_0}^2(v))$. To generate points on the curve for negative values of α, the eigenvector corresponding to the smallest eigenvalue of $(1-\beta)P_{u_0}^2 + \beta L$ was found for $\beta \in [0, 1]$.

The results are shown in Figure 3. As predicted, both constructions result in wavelets that obey the computed bound. The spectral graph wavelets are further from the bound, and get closer to the bound at high spectral spreads. The diffusion wavelets track the bound very closely, and do so more closely at lower spectral spreads. Of course, there are other factors in evaluating wavelet transforms on graphs: oversampling ratio, computational complexity (of both forward and inverse transforms,) and conditioning are very important.

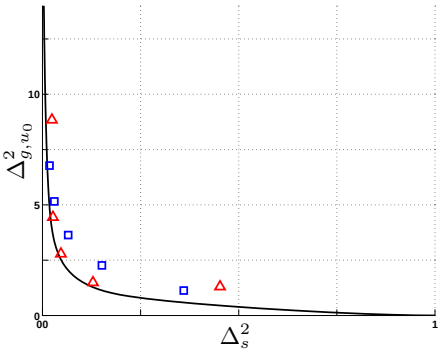

Fig. 3. Spectral spread versus graph spread on a graph based on the "Swiss roll" dataset. Solid line: computed curve $\gamma(s)$. Squares: spectral graph wavelets [8]. Triangles: diffusion wavelets [6].

5. CONCLUSIONS

In this paper we described metrics for signals on graphs that quantify precisely how well-localized they are in the graph and spectral domains. These metrics can be used to evaluate the performance of existing wavelet transforms in the literature. We further described a scheme for bounding the localization in both domains, and compared a few existing wavelet transforms on graphs to the new bounds.

6. REFERENCES

[1] M. Vetterli and J. Kovačević, *Wavelets and Subband Coding*. Englewood Cliffs, NJ: Prentice Hall, 1995.

[2] M. Belkin, "Problems of learning on manifolds," Ph.D. dissertation, University of Chicago, Chicago, Illinois, 2003.

[3] E. Giné and V. Koltchinskii, "Empirical graph Laplacian approximation of Laplace-Beltrami operators: Large sample results," *IMS Lecture Notes-Monograph Series*, vol. 51, pp. 238–259, 2006.

[4] P. Milanfar, "A tour of modern image filtering," *To Appear in IEEE Signal Processing Magazine*, 2011.

[5] H. Hoppe, "Progressive meshes," in *Proc. SIGGRAPH*, 1996, pp. 99–108.

[6] R. R. Coifman and M. Maggioni, "Diffusion wavelets," *Applied and Computational Harmonic Analysis*, vol. 21, no. 1, pp. 53–94, Jul. 2006.

[7] W. Wang and K. Ramchandran, "Random multiresolution representations for arbitrary sensor network graphs," in *Proc. Int. Conf. on Acoustics, Speech, and Signal Proc.*, 2006.

[8] D. Hammond, P. Vandergheynst, and R. Gribonval, "Wavelets on graphs via spectral graph theory," *Applied and Computational Harmonic Analysis*, vol. 30, pp. 129–150, Mar. 2011.

[9] S. Narang and A. Ortega, "Local two-channel critically sampled filter-banks on graphs," in *Proc. IEEE International Conference on Image Processing (ICIP)*, 2010, pp. 333–336.

[10] A. Agaskar and Y. M. Lu, "An uncertainty principle for functions defined on graphs," in *Proc. SPIE Conference on Wavelets and Sparsity*, San Diego, CA, 2011.

[11] ——, "Uncertainty principles for signals defined on graphs," *to be submitted*, 2011.

[12] F. R. K. Chung, *Spectral graph theory*. Providence, RI: American Mathematical Society, 1997.

[13] P. Lancaster and M. Tismenetsky, *The theory of matrices: with applications*, 2nd ed. New York: Academic Press, 1985.